

# Scaling theory of supermolecular structures in block copolymer–solvent systems:

## 1. Model of micellar structures

T. M. Birshtein and E. B. Zhulina

*Institute of Macromolecular Compounds of the Academy of Sciences of the USSR, Leningrad, USSR*

*(Received 2 March 1988; accepted 31 May 1988)*

The micellar structures formed by two-block copolymers in a block copolymer–solvent system were considered by using the scaling method. The equilibrium parameters of micelles were determined depending on the composition of the copolymer and the strength and concentration of the solvent in the system. It was shown that a 'quasiglobular' regime exists in a micellar solution at concentrations exceeding that of overlapping of individual micelles. The results of the theory are compared with the experimental results.

**(Keywords: scaling theory; block copolymer; solvent systems; micellar structures)**

### INTRODUCTION

A characteristic feature of two- (or three-) block copolymers is known to be micro-phase separation and the formation of supermolecular structures with segregated components: individual micelles in dilute solutions in selective solvents and regular superstructures with various morphologies at a high concentration of the block copolymer. The physical bases of structure formation are both the poor solubility of one of the components of the block copolymer and the incompatibility of its components. In relatively dilute solutions the poor solubility of the component forming the micelle core predominates. The soluble crown consisting of the second component retains the micelle in solution. At a high concentration of the copolymer the main factor determining the supermolecular structure becomes the incompatibility of copolymer components, leading to micro-phase separation. The resulting supermolecular structures in solution may be treated as liquid-crystalline structures.

Many papers have already been published on the equilibrium theory of structure formation in block copolymer systems, in particular papers by Meier<sup>1</sup> and Helfand and Wasserman<sup>2</sup>. They have been carried out to the approximation of the self-consistent field and mainly deal with the conditions of high concentration of the block copolymer under which this approximation is valid.

The success of the scaling concepts in describing the solutions of linear homopolymers and the mathematical simplicity and clearness of the physical picture make the scaling approach a very useful tool for the analysis of a number of more complex polymer systems. In this and a forthcoming paper, the scaling approach is used for the analysis of supermolecular structures in a broad class of two-block copolymer–solvent systems. A single method will be used to obtain a general picture of equilibrium structure formation ranging from isolated micelles in dilute solutions in selective solvents to the superstructures (liquid crystalline structures) with different morphologies

at a high concentration of the block copolymer. The dependences of the morphology and the thermodynamic and geometric characteristics of these structures on molecular parameters (molecular weight of the blocks, copolymer composition, strength and concentration of the solvent) will be investigated. Some results for individual classes of structures have been published earlier<sup>8–10</sup>.

Although this theory is based on a simplified approach (only the main contributions to the free energy of the system, with only the power dependences on parameters and without the numerical coefficients, have usually been taken into account), the results of the theory were found to be in surprisingly good agreement with a large amount of experimental data in the literature. This will be shown in this and a subsequent paper. This agreement also serves as a confirmation of the physical assumptions on which this model is based.

### THEORY

#### *Initial characteristics of the model*

A system containing a solvent and a two-block copolymer  $A_{N_A}B_{N_B}$  with incompatible components A and B will be considered. Let us suppose that:

(1) Components A and B are flexible-chain polymers with approximately the same flexibility (parameters of segment asymmetry  $p = l/a \approx 1$ , where  $l$  is the persistent length and  $a$  is the chain thickness). In principle, it is possible to take chain stiffness into account,  $p_A, p_B > 1$ , by using the diagram of state of the solution of the corresponding homopolymers<sup>3,4</sup>.

(2) The numbers of units (chain parts of length  $a$  equal to the chain thickness) are large,  $N_A, N_B \gg 1$ , which ensures the applicability of the scaling asymptotic relationships.

(3) The system is in equilibrium.

(4) The conditions of formation of the supermolecular structure with segregated components have been obeyed.

In dilute solutions, the solvent is assumed to have maximum selectivity: it is a good ( $\tau_A = (T - \theta_A)/T \approx 1$ ) or a  $\theta$  ( $\tau_A = 0$ ) solvent for block A and a precipitant for block B ( $\tau_B = (T - \theta_B)/T < 0$ ), from which it is completely excluded. In more concentrated systems, the formation of regular superstructures is determined by the incompatibility of the components. In this case the requirements for the selectivity of the solvent are not imposed and the solvent concentration in blocks A and B is considered to be fixed.

(5) The dependences of the characteristics of the system on  $\tau$  will not be considered and it will be assumed that under conditions of a good solvent  $\tau = 1$ . This restriction is not essential: the power dependences on  $\tau_A$  and  $\tau_B$  can readily be obtained in the proposed scheme. They have been omitted only to simplify the formulae.

(6) We will consider the superstructures of different morphology (subscript  $i$ ): at  $i = 1$  the structural elements are lamellae, at  $i = 2$  they are cylinders and at  $i = 3$  they are spheres (Figure 1).

(7) The interphase layer between the A and B elements of the structure is narrow, i.e. its thickness  $\Delta$  is small compared with the size of the elements A and B and is, just as its structure is, independent of the molecular weights of the blocks. In this case the thermodynamic characteristic of the interphase layer is the surface tension coefficient  $\gamma$  or the relative characteristic  $\phi = \gamma a/kT$ , where  $\gamma, \phi = \text{const.} \times (N_A, N_B)$  and depend only on the chemical structure of the components A and B and solvent concentration.

#### Free energy of the system

The equilibrium thermodynamic and geometric characteristics of the polymer chain in a structure with a given morphology  $i$  are determined by the minimization of its

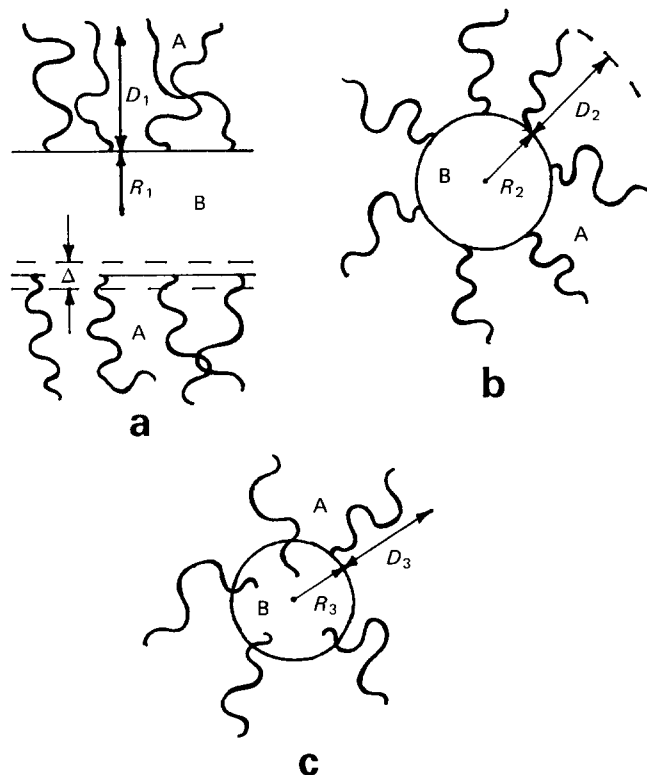


Figure 1 Scheme of micellar structures with (a) lamellar ( $i = 1$ ); (b) cylindrical ( $i = 2$ ) and (c) spherical ( $i = 3$ ) morphologies

conformational free energy  $\Delta F^i$ , which is given by

$$\Delta F^i = \Delta F_A^i + \Delta F_B^i + \Delta F_S^i \quad (1)$$

where  $\Delta F_A^i$  and  $\Delta F_B^i$  are the conformational free energies of the A and B blocks in the corresponding structural elements and  $\Delta F_S^i$  is the surface free energy. In each term, only the main contribution with the power dependence (in some cases the logarithmic dependence) on the parameters will be taken into account. The numerical coefficients have been omitted.

Let us consider the terms in equation (1), writing the free energy in  $kT$  units. For definiteness, let us consider an isolated micelle in a selective solvent completely excluded from block B. The surface free energy  $\Delta F_S^i$  is determined by the relative surface tension coefficient  $\phi = \gamma a/kT$  and the specific (per chain) surface area  $\sigma_i$  as follows:

$$\Delta F_S^i = \phi \sigma_i \quad (2)$$

and decreases with the decrease of  $\sigma_i$ . This tendency is opposed by simultaneous increasing stretching of blocks A and B in their structural elements and by increasing concentration of the soluble A units in the micelle crown:

$$\Delta F_A^i = \Delta F_{A,el}^i + \Delta F_{A,conc}^i \quad (3)$$

$$\Delta F_B^i = \Delta F_{B,el}^i \approx R_i^2/a^2 N_B \quad (4)$$

Equation (4) takes into account the stretching of blocks B from the undisturbed Gaussian size  $R_B \approx a N_B^{1/2}$  (corresponding to the conditions of high volume concentration  $c_B \approx 1$ ) to the size  $R_i$  of the B element in the structure with morphology  $i$ .

As to the soluble A blocks, within the approximation of the narrow interphase layer  $\Delta \ll R_i$ , they may be considered to be chains consisting of  $N_A$  units 'grafted' at one end onto an impermeable interphase surface with grafting density  $1/\sigma_i$ . Let this layer of grafted chains immersed in the solvent be called free. Its characteristics are considered in the next section and will be used in further discussion.

#### Free layer of grafted chains

Many papers have been published on the scaling analysis of the free layer of flexible polymer chains consisting of  $N_A \gg 1$  units grafted onto an impermeable planar ( $i = 1$ )<sup>5-7</sup>, cylindrical ( $i = 2$ )<sup>8</sup> or spherical ( $i = 3$ )<sup>8-10</sup> matrix, i.e. the matrix with the dimensionality  $i_M = 3 - i$ . The layer characteristics were found by minimization of the free energy according to equation (3), the terms of which were determined on the basis of the temperature-concentration diagram of the solution of linear polymers<sup>3</sup>.

Figure 2 shows the diagrams of state of the layers obtained in References 8-10 and Table 1 gives the power

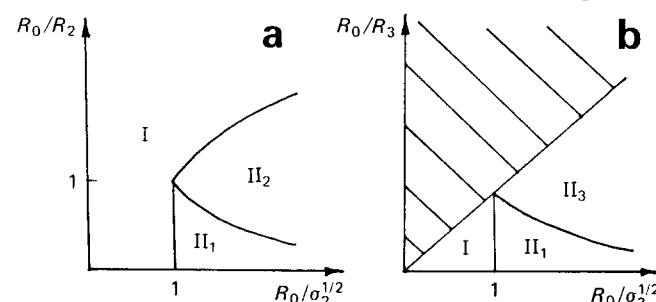


Figure 2 Diagram of state of a free layer of chains grafted onto (a) cylindrical ( $i = 2$ ) and (b) spherical ( $i = 3$ ) surfaces of radius  $R$  at a density of  $1/\sigma$ . Shaded area corresponds to the non-physical values of the parameter  $f_3 < 1$ . The layer characteristics in each region are given in Table 1. The equations of the boundaries are:  $R_0 \approx \sigma_i^{1/2} (I-II_1)$ ;  $R_i \approx D_i (II_1-II_2)$ ;  $R_0 \approx D_2 (I-II_2)$

Table 1 Power dependences of parameters of a grafted chain layer

	I	II <sub>1</sub>	II <sub>2</sub>	II <sub>3</sub>
$\lambda/a$	$N_A^\lambda$	$N_A \left(\frac{\sigma}{a^2}\right)^{(v-1)/2v}$	$f_2^{(1-v)/(1+v)} N_A^{2v/(1+v)}$	$N_A^\lambda f_3^{(1-v)/2}$
$\lambda$	$N_A^{1-v} \left(\frac{\sigma}{a^2}\right)^{-1}$	$\left(\frac{\sigma}{a^2}\right)^{(1-3v)/2v}$	$f_2^{(3v-1)/2v} \left(\frac{r}{a}\right)^{(1-3v)/2v}$	$f_3^{(3v-1)/2v} \left(\frac{r}{a}\right)^{(1-3v)/v}$
$\lambda/a$	$N_A^\lambda$	$\left(\frac{\sigma}{a^2}\right)^{1/2}$	$f_2^{-1/2} \left(\frac{r}{a}\right)^{1/2}$	$f_3^{-1/2} \left(\frac{r}{a}\right)$

dependencies of layer characteristics under the different regimes of the diagrams. The following symbols are used:  $R_i$  is the radius of the matrix curvature; in the limit  $R_i \rightarrow \infty$  ( $i=2, 3$ ) we obtain the planar ( $i=1$ ) layer;  $a_0 = aN_A^v$  is the size of an isolated A block under the conditions of a good ( $v=3/5$ ) or a  $\theta$ -solvent ( $v=1/2$ );  $\sigma_i$  is the surface density of grafting ( $i=1, 2, 3$ ); the characteristic values depending on morphology are  $f_i$ , here  $f_1 = 1/\sigma_1$  is the surface grafting density under the conditions of a planar layer;  $f_2 = 2R_2/\sigma_2^{1/2}$  is the linear grafting density in a cylindrical layer (chain number per unit length);  $f_3 = R_3^2/\sigma_3$  is the angular grafting density in a spherical layer (chain number per unit solid angle);  $\lambda = 4\pi f_3' > 1$  is the total chain number in a spherical layer.

It can be seen from Figure 2 that for cylindrical and spherical matrices ( $i=2, 3$ ) the diagram of state contains three regimes. Region I corresponds to widely spaced grafting,  $\sigma_i^{1/2} > R_0$ , of non-overlapping chains forming individual coils. On chain overlapping, a single layer of geometry  $i$  is formed (regimes II<sub>*i*</sub>). It can be seen from Figure 2 that at any matrix geometry a regime of the planar layer, II<sub>1</sub>, exists. If  $R_0/R_i \neq 0$  it can occur at not very large  $R_0/\sigma_i^{1/2}$ , i.e. not for very long and for relatively seldom grafted chains, when the layer height  $D_i$  (radial chain dimension in a layer) is small compared with the radius of the matrix curvature,  $R_0 < D_i < R_i$ , and the chains do not 'feel' the curvature of the surface. For a planar matrix  $R_1 \rightarrow \infty$ ,  $R_0/R_2 = R_0/R_3 = 0$ , i.e. the  $x$ -axis in Figure 2, we always have  $D_1 > R_1$ , and regime II<sub>1</sub> is not limited from above. For the cylindrical and spherical matrices to the right of II<sub>1</sub> regime II<sub>*i*</sub> ( $i=2, 3$ ) occurs in the diagrams of state. Under this regime the geometry and thermodynamics of the layer reflect the geometry of the matrix.

The main characteristic of layers under various regimes reduce to the following (Table 1):

(1) Local correlations of layer density in a planar layer regime II<sub>1</sub>) correspond to those in a three-dimensional dilute solution of constant concentration. The correlation radius  $\xi$  of density is constant throughout the layer height.

To avoid misunderstanding it should be noted that only the absence of the power dependence  $c(r) \sim r^0$  ( $r$  is the distance from the matrix) is meant by the constancy of concentration in a planar layer. The decrease in  $c(r)$  with increasing  $r$  occurring according to several papers<sup>11-13</sup> is not expressed by a power function and does not affect the power dependences in Table 1 and equation (5), influencing only the numerical coefficients (which are not taken into account in our consideration).

(2) Chains in a planar layer are extended and their size perpendicular to the matrix is  $D \sim N$ . This corresponds

to a completely extended sequence of blobs with a radius  $\xi$  belonging to each chain.

(3) In spherical and cylindrical matrices (regimes II<sub>*i*</sub>,  $i=2, 3$ ), the effective area per chain increases according to a power law with increasing distance from the matrix. This leads to a power decrease in unit density  $c(r) \sim r^{-(3v-1)/2v}$  at  $i=2$  and  $c(r) \sim r^{-(3v-1)/v}$  at  $i=3$  (in contrast to  $c(r) \sim r^0$  at  $i=1$ ), and to a power decrease in chain extension and increase in the correlation radius  $\xi(r)$  with increasing distance from the matrix.

(4) The free energy of the grafted chain in a layer under regime II<sub>*i*</sub>

$$\Delta F_A^i \simeq \begin{cases} N_A \sigma_1^{-v/2} & i=1 & (5a) \\ N_A^{v/(1+v)} f_2^{1/(1+v)} & i=2 & (5b) \\ f_3^{1/2} \ln(D_3/R_3) & i=3 & (5c) \end{cases}$$

decreases when the geometry of the layer changes from planar ( $i=1$ ) to cylindrical and spherical ( $i=3$ ) geometry. Thus  $\Delta F_A^1$  is proportional to  $N_A$ ;  $\Delta F_A^2 \sim N_A^{v/(1+v)}$  and in the spherical layer only a weak logarithmic dependence of  $\Delta F_A^3$  on  $N_A$  exists (via  $D_3$ ):  $\Delta F_A^3 \sim N^0$ . The reason for this is that the decrease in the concentration  $c_A(r)$  of units to the periphery of the layer becomes more marked on passing from  $i=1$  to  $i=3$  (see Table 1).

The above data will be used for analysis of the structures of block copolymers in the next section.

## RESULTS

### Isolated micelles with a dense core

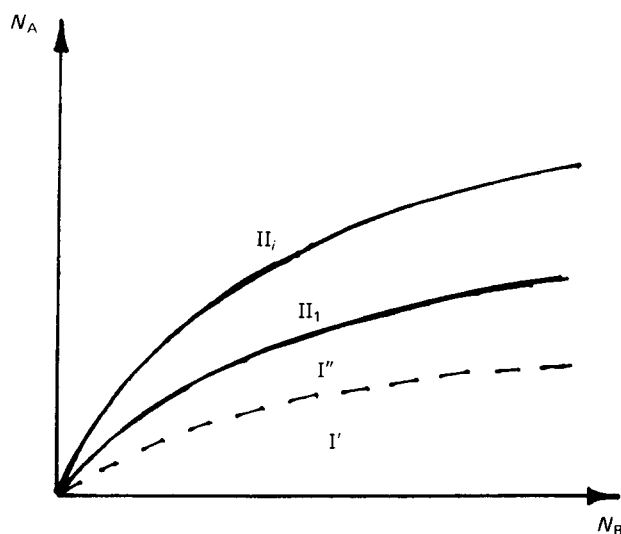
Equations (1)–(5) contain all the information necessary for the determination of equilibrium characteristics of micelles by the minimization of  $\Delta F^i$ . Table 2 (see also Table 3) gives the equilibrium parameters of cylindrical and spherical micelles,  $i=2, 3$  obtained under different regimes of the diagram of state shown in Figure 3. Three regimes are singled out in Figure 3. They exist consecutively with increasing  $N_A/N_B$  ratio and correspond to the three regimes of behaviour of grafted chain layers at  $i=2$  and 3 (Figure 2).

Regime I consists of isolated (I') or slightly overlapping (I'') coils A grafted onto a dense core consisting of B units. The layer structure is determined by a compromise between  $\Delta F_A^i$  from equation (2) and  $\Delta F_B^i$  from equation (4) since  $\Delta F_A^i < \Delta F_B^i$ . As a result, such micelle characteristics as specific surface area  $\sigma_i$ , core size  $R_i$  and number of chains  $f_i$  do not depend on  $N_A$ , and their molecular-weight dependence is determined only by  $N_B$ .

Regime II<sub>1</sub> is the planar regime for the A blocks, possible at any micelle geometry when the thickness  $D$  of the crown consisting of A blocks is less than the size  $R_i$  of the core consisting of B blocks. For both spherical and cylindrical micelles, regime II<sub>1</sub> exists at  $N_A/N_B < 1$

**Table 2** Power molecular weight dependence of equilibrium parameters of isolated cylindrical and spherical micelles

Regime	Polymer composition	$\sigma_i/a^2; \frac{\Delta F^i}{\phi}$		$R_i/a$		$D_i/a$		$f_i$	
		$i=2$	$i=3$	$i=2$	$i=3$	$i=2$	$i=3$	$i=2$	$i=3$
I'	$N_A < N_B^{1/6\nu}$						$N_A^\nu$		$N_B$
I''	$N_B^{1/6\nu} < N_A < N_B^{(1+2\nu)/6\nu}$		$N_B^{1/3}$				$N_A N_B^{(\nu-1)/6\nu}$		$N_B$
II <sub>1</sub>	$N_B^{(1+2\nu)/6\nu} < N_A < N_B^{(1+2\nu)/5\nu}$	$N_A^{2\nu/(1+2\nu)}$		$N_B^{2/3} \phi^{1/3}$			$N_A^{3\nu/(2\nu+1)}$	$N_B N_A^{-4\nu/(1+2\nu)}$	$N_B^2 N_A^{-6\nu/(1+2\nu)}$
II <sub>2</sub>	$N_A > N_B^{(1+2\nu)/5\nu}$	$N_A^{\nu/(3+\nu)} N_B^{1/(3+\nu)}$		$N_B^{(2+\nu)/(3+\nu)} N_A^{-\nu/(3+\nu)}$			$N_B^{(1-\nu)/(3+\nu)} N_A^{4\nu/(3+\nu)}$	$N_B^{(1+\nu)/(3+\nu)} N_A^{-2\nu/(3+\nu)}$	
II <sub>3</sub>			$N_B^{2/5}$		$N_B^{3/5}$		$N_B^\nu N_B^{2(1-\nu)/5}$		$N_B^{4/5}$


**Figure 3** Diagram of state of an isolated micelle with morphology  $i$ . The micelle characteristics in each region are given in Table 2. The equations of the boundaries are:  $N_A \approx N_B^{1/6\nu}$  (I'-II'');  $N_A \approx N_B^{(2\nu+1)/6\nu}$  (I''-II<sub>1</sub>);  $N_A \approx N_B^{(2\nu+1)/5\nu}$  (II<sub>1</sub>-II<sub>i</sub>)

over a relatively narrow range:  $N_A/N_B \sim N_A^{-\alpha}$  where  $\alpha$  varies from 0.39 to 0.27, under the conditions of a good solvent for the soluble A blocks, and from 0.33 to 0.20, under the conditions of a  $\theta$ -solvent (Table 2). Only for a planar lamella is regime II<sub>1</sub> retained with an unlimited growth in  $N_A/N_B$ . Under regime II<sub>1</sub>,  $\Delta F_A^i > \Delta F_B^i$ , the micelle characteristics are determined by a compromise between  $\Delta F_S^i$  from equation (2) and  $\Delta F_A^i$  from equation (5) and, correspondingly,  $\sigma_i$ ,  $R_i$  and  $f_i$  acquire a power dependence on  $N_A$ : at a fixed  $N_B$  the core size  $R_i$  and the chain number  $f_i$  decrease and  $\sigma_i$  increases with increasing  $N_A$ .

At higher  $N_A/N_B$ , regimes II<sub>i</sub> ( $i=2, 3$ ) exist. Under these regimes the behaviour of the A blocks is related to the micellar geometry, i.e. the curvature of the core surface becomes apparent and, correspondingly, the space accessible to the A chains increases. The micellar structure is determined by the competition of contributions of  $\Delta F_S^i$  from equation (2) and  $\Delta F_A^i$  from equation (5b) or (5c). For spherical micelles ( $i=3$ ) when  $\Delta F_A^3$  only logarithmically depends on  $N_A$ , the power dependence of  $R_3$ ,  $f_3$  and  $\sigma_3$  on  $N_A$  disappears, being replaced by a weak logarithmic dependence (which is not given in Table 2 and is contained in the factor  $x_0 = \ln(D_3/R_3)$  in Table 3). This factor depends on the exponent  $\nu$  characterizing the strength of the solvent for the A blocks. For cylindrical micelles ( $i=2$ ), the dependence of  $R_2$ ,  $f_2$  and  $\sigma_2$  on  $N_A$  also becomes weaker, though remaining a power form.

**Table 3** Power dependence of characteristics of spherical micelles in various ranges of solution concentration

	Region 0 $c_A < c_A^*$	Region I $c_A^* < c_A < c_A^{**}$	Region II $c_A > c_A^{**}$
$f$	$\left(\frac{\phi}{x_0}\right)^{6/5} N_B^{4/5}$	$\left(\frac{\phi}{x}\right)^{6/5} N_B^{4/5}$	$\phi N_B c_A^{\nu(3\nu-1)}$
$R/a$	$\left(\frac{\phi}{x_0}\right)^{2/5} N_B^{3/5}$	$\left(\frac{\phi}{x}\right)^{2/5} N_B^{3/5}$	$\phi^{1/3} N_B^{2/3} c_A^{\nu(3\nu-1)}$
$D/a$	$\left(\frac{\phi}{x_0}\right)^{6/25} N_B^{3/5} N_A^{4/25}$	$\left(\frac{\phi}{x}\right)^{2/5} N_A^{1/3} N_B^{4/15} c_A^{-1/3}$	$\phi^{1/3} N_A^{1/3} N_B^{1/3} c_A^{-(1-2\nu)/3(3\nu-1)}$

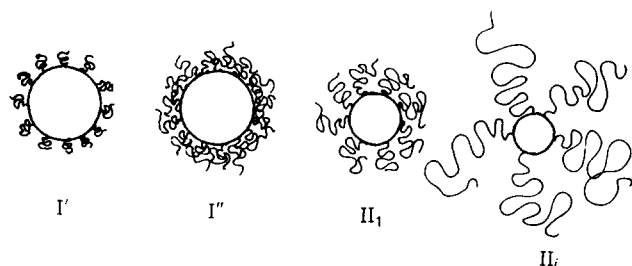

**Figure 4** Change in equilibrium parameters of a spherical micelle with increasing  $N_A$  ( $N_B = \text{const.}$ )

Figure 4 shows schematically the change in micelle size resulting from an increase in  $N_A$  at  $N_B = \text{constant}$ . In this case transition between regimes I'  $\rightarrow$  I''  $\rightarrow$  II<sub>1</sub>  $\rightarrow$  II<sub>i</sub> ( $i=2, 3$ ) takes place. As can be seen from the data in Table 2, this transition involves, apart from the evident increase in the thickness  $D$  of the soluble crown, a decrease in the number of inner blocks B composing the core and their degree of extension. For spherical micelles, however, these blocks remain extended:  $R_3 > aN_B^{1/2}$  under all regimes. In cylindrical micelles in regime II<sub>2</sub> at  $N_A \approx N_B^{(1+2\nu)/2\nu}$  the size of the core becomes equal to that of the unperturbed B block  $R_2 \approx aN_B^{1/2}$ . When  $N_A$  increases further, the stretching of inner blocks is replaced by their compression.

In contrast to the inner blocks, the stretching,  $D/aN_A^\nu$ , of the outer A blocks increases with the transition I'  $\rightarrow$  I''  $\rightarrow$  II<sub>1</sub>  $\rightarrow$  II<sub>i</sub>. They begin to stretch markedly under regime I'. Under regime II<sub>2</sub> (cylindrical micelles), their degree of extension according to the power laws depends on  $N_A$  and  $N_B$ , whereas under regime II<sub>3</sub> (spherical micelles) it is mainly determined by the value of  $N_B$ , only logarithmically increasing with  $N_A$  (Tables 2 and 3).

It is noteworthy that the core size of the spherical micelles under regime II<sub>3</sub> is determined by the well known expression  $R_3 \approx aN_B^{3/5}$ . This coincidence of the exponents for the inner block in a dense core with that for a free chain is merely fortuitous. In fact, these results are a consequence of the minimization of free energies repre-

sented as a sum of two terms. The structure and the physical meaning of these terms are fundamentally different for the isolated chain and for a chain in the micelle core, and only the results of minimization coincide:

$$\Delta F (\text{free chain}) = \frac{R_0^2}{a^2 N_B} + \frac{N_B^2 a^3}{R_0^3} \rightarrow R_0 \simeq a N_B^{3/5} \quad (6)$$

$$\begin{aligned} \Delta F (\text{micelle}) &= \Delta F_S + \Delta F_A = \phi \frac{R_3^2}{f_3} + f_3^{1/2} \\ &= \frac{\phi N_B}{R_3} + \frac{R_3^{3/2}}{N_B^{1/2}} \rightarrow R_3 \simeq a N_B^{3/5} \end{aligned} \quad (7)$$

Equation (7) takes into account equations (1)–(3) and (5c) and the evident ratio for the core density  $f_3 = R_3^3/a^3 N_B$ .

The structure of the soluble crown in a spherical micelle under regime II<sub>3</sub> will now be considered. It follows from Table 1 that the density of units  $c_A(r)$  in the crown decreases according to the power law from the core surface  $r = R_3$  to its periphery  $r = R_3 + D \simeq D$  (under regime II<sub>3</sub> we have  $D > R_3$ ):

$$c_A(r) \simeq f_3^{(3\nu-1)/2\nu} r^{-(3\nu-1)/\nu} \quad (8)$$

Denoting these limiting values of  $c_A$  by  $c_A^*$  and  $c_A^{**} > c_A^*$  and applying the data from Table 2, we obtain

$$c_A^* = c_A(D) \simeq f_3^{(3\nu-1)/2} N_A^{-(3\nu-1)} \simeq (N_B^{2/5} N_A^{-1})^{3\nu-1} \quad (9)$$

$$c_A^{**} = c_A(R_3) \simeq f_3^{(3\nu-1)/4\nu} \simeq N_B^{-(3\nu-1)/5\nu} \quad (10)$$

To the approximation used it should be noted that the concentration  $c_A^*$  coincides with the average concentration  $\bar{c}_A$  of A units in the micelle crown:

$$\bar{c}_A \simeq N_A a^3 f_3 / D^3 \simeq c_A^* \quad (11)$$

Equations (9) and (10) show that not only the maximum concentration of units  $c_A^{**}$  in the crown but also the minimum concentration  $c_A^*$  on the periphery of the crown exceeds the concentration of units in the free A coil,  $c_A \sim N_A^{-(3\nu-1)}$ .

It is useful for further discussion to represent the free energy of the crown of the spherical micelle (equation (5c)) by the concentrations  $c_A^*$  and  $c_A^{**}$ . Applying equation (8) we have

$$\Delta F_A^3 \simeq f_3^{1/2} x_0 \quad (12)$$

where

$$x_0 = \ln(D_3/R_3) \simeq \ln\left(\frac{c_A^{**}}{c_A^*}\right) \sim \ln(N_A N_B^{(2\nu-1)/5\nu}) \quad (13)$$

#### Micelles in a selective solvent: structure and interaction

In the preceding section the characteristics of isolated micelles with different morphologies have been considered. In the investigation of a block copolymer in solution the question arises what are the conditions of formation of soluble micellar structures. For micelle formation, the volume concentration of the block copolymer in solution should evidently exceed a certain critical concentration  $c_c$ . At  $c < c_c$  supermolecular structures are not formed and insoluble blocks B form intramolecular globular structures (see Reference 14).

Let us assume that the condition  $c > c_c$  is obeyed, leaving outside the scope of this paper the problem of establishing the relationship between  $c_c$  and the molecular characteristics. The problem of conditions of micelle

solubility will not be discussed either. It will only be noted that solubility increases with the ratio of the length of the soluble block to that of the insoluble block,  $N_A/N_B$ . Hence the most definite case of micelle formation is that of block copolymers with  $N_A > N_B$ , and we restrict ourselves to considering this case in the present section.

The results reported in the preceding section permit a comparison of the relative stability of micelles with different morphologies, i.e. cylindrical (regime II<sub>2</sub>) and spherical (regime II<sub>3</sub>) micelles which can be formed by chains with  $N_A > N_B^{(1+2\nu)/5\nu}$ . It can be seen that the spherical micelles are preferable because the conformational free energy of their chains is lower than that in cylindrical micelles,  $\Delta F^3 < \Delta F^2$ . The advantage of spherical micelles is also enhanced by the contribution of combinatorial entropy in which micelle distribution in solution is taken into account:

$$\Delta s_i = \ln \frac{c}{N} - \frac{1}{P_i} \ln \frac{c}{P_i N} \quad (14)$$

where  $c$  is the volume concentration of the block copolymer in solution,  $N = N_A + N_B$  and  $P_i$  is the total number of chains in a micelle ( $P_3 = f_3$  and  $P_2 = f_2 y$ , where  $y$  is the length of the cylindrical core).

It is evident that  $P_2 > P_3$ , so that  $\Delta s_3 > \Delta s_2$ . It follows from these results that block copolymers with  $N_A > N_B$  should form spherical micelles, and in this section only these micelles will be considered.

Note that the tendencies to the formation of spherical (and not cylindrical) micelles is evidently retained for block copolymers with  $N_A < N_B$  (regimes I and II<sub>1</sub>). Indeed, the conclusion that  $\Delta s_3 > \Delta s_2$  depends only on the geometry of the micelle and does not depend on the regime of behaviour of its outer layer, whereas the conformational free energies under regimes I and II<sub>1</sub> are independent of the geometry  $\Delta F^2 \simeq \Delta F^3$  (within the approximation used). However, the difference between  $\Delta s_2$  and  $\Delta s_3$  is not large and, consequently, for  $N_A < N_B$ , quantitative analysis of  $\Delta F$ , taking into account numerical coefficients and also (as indicated above) analysis of conditions of micelle solubility, is needed.

Let us now consider a solution of spherical micelles (subscript  $i=3$  will be omitted) formed by the chains of the block copolymer with  $N_A > N_B$  (concentration of the block copolymer in solution  $c > c_c$ ) and let us increase the concentration  $c$  of the block copolymer. The concentration of soluble units  $c_A$  will be taken to be the measure of this concentration:

$$c_A = c N_A / (N_A + N_B) \simeq c$$

According to the usual concepts of the scaling theory of solutions, at  $c_A < \bar{c}_A \simeq c_A^*$  (equations (9) and (11)), we evidently have a dilute solution of isolated micelles. Their characteristics are independent of the solution concentration  $c_A$  (as usual, the absence of power dependence is meant). They have been considered in the preceding section and are also listed in Table 3.

At  $c_A > c_A^*$ , the soluble crowns begin to interact with each other. In the concentration range  $c_A^* < c_A < c_A^{**}$ , it is possible to apply the model and approach developed for a similar system, a semi-dilute star solution<sup>15,16</sup>. According to Reference 15 (see detailed discussion in that reference), a double-layer model of the micelle crown will be assumed, i.e. the crown is divided into two layers. The unperturbed inner layer retains the structure of an isolated micelle. The perturbed outer layers of micelles

appear to be a semi-dilute solution at a concentration  $c_A$ . The density profile of the A units (with respect to the micelle centre) is given by

$$c_A(r) \simeq \begin{cases} f^{(3\nu-1)/2\nu} \left(\frac{r}{a}\right)^{-(3\nu-1)/\nu} & R < r < \rho \\ c_A & r < \rho \end{cases} \quad (15)$$

where  $\rho$  is the size of the inner unperturbed part of the crown determined by the crossover of equations (15):

$$\rho \simeq a f^{1/2} c_A^{-\nu/(3\nu-1)} \quad (16)$$

The number,  $f$ , of chains in a micelle in this region of concentration may, generally, be a function of  $c_A$ .

The free energy of the A block will be represented as a sum of the inner layer ( $r < \rho$ ) and outer layer ( $r > \rho$ ) components:

$$\Delta F_A = \Delta F_A^{\text{in}} + \Delta F_A^{\text{ex}} \quad (17)$$

which, as before, contain the elastic and the concentration contributions:

$$\begin{aligned} \Delta F_A^{\text{in}} &= \Delta F_{A,\text{el}}^{\text{in}} + \Delta F_{A,\text{conc}}^{\text{in}} \\ \Delta F_A^{\text{ex}} &= \Delta F_{A,\text{el}}^{\text{ex}} + \Delta F_{A,\text{conc}}^{\text{ex}} \end{aligned} \quad (18)$$

Since the inner part of the crown is assumed to be unperturbed, equations (5c), (12) and (13) remain valid for the intramicellar free energy

$$\Delta F_A^{\text{in}} \simeq f^{1/2} \ln \frac{\rho}{R} \simeq f^{1/2} \ln \left( \frac{c_A^{**}}{c} \right) \simeq f^{1/2} x \quad (19)$$

where  $x \equiv \ln(c_A^{**}/c_A)$ .

To evaluate the outer component, it should be recollected that (as has been shown for a semi-dilute star solution) at  $c > c^*$  the outer perturbed parts of the branches retain the residual extension, decreasing with increasing concentration up to a concentration equal to  $f^{2\nu} c_A^*$  (regime III in diagrams in Reference 15). Comparison of values of  $c_A^*$  and  $c_A^{**}$  in equations (9) and (10) shows that, if in the block copolymer we have  $N_B > N_A^{5\nu/(1+8\nu)} \approx N_A^{1/2}$ , then the condition  $c_A^{**}/c_A^* < f^{2\nu}$  is fulfilled and hence in the concentration range  $c_A^* < c_A < c_A^{**}$ , the outer parts of the A chains remain extended. It will be assumed, according to Reference 15, that the solution structure reduces this extension to the minimum possible value, i.e. that micelles are segregated and their outer layers do not overlap.

To evaluate the energy of elastic extension,  $\Delta F_{A,\text{el}}^{\text{ex}}$  of the parts of the A blocks in the outer layer, let us consider this layer (semi-dilute solution at a concentration  $c_A$ ) as a melt of chains consisting of blobs and attached by one end to a sphere of radius  $\rho$  (Figure 5). The size of each blob is  $\xi_A \simeq a c_A^{-\nu/(3\nu-1)}$ . The requirement of constant concentration  $c_A$  in a layer implies that the grafted chains are extended non-uniformly: near the sphere extension is more pronounced than on the periphery of the layer. It will be assumed, according to the method used in Reference 17, that the local extension of a chain part of  $\delta n$  blobs by a distance  $\delta r$  is described by the Gaussian term

$$\delta F_{\text{el}}(\delta n) \simeq \frac{(\delta r)^2}{\xi_A^2 \delta n} \quad (20)$$

The summation of  $\Delta F(\delta n)$  over  $n$  and the application of the condition of dense filling up of the outer layer by its

blobs (micelle impermeability)

$$f \delta n \xi_A^3 \simeq r^2 \delta r \quad (21)$$

gives

$$\Delta F_{A,\text{el}}^{\text{ex}} \simeq f \xi_A \left( \frac{1}{\rho} - \frac{1}{D} \right) \simeq \frac{f \xi_A}{\rho} \simeq f^{1/2} \quad (22)$$

where  $D(c_A)$  is the size of the outer layer and  $D > \rho$ ; see equation (16).

The concentration component  $\Delta F_{A,\text{conc}}^{\text{ex}} \simeq N_A c_A^{1/(3\nu-1)}$  is independent of the micelle parameters and hence does not take part in subsequent minimization.

It can be seen from equations (19) and (22) that  $\Delta F_{A,\text{el}}^{\text{ex}} < \Delta F_A^{\text{in}}$  so that at  $c_A^* < c_A < c_A^{**}$  the total  $\Delta F_A$  value is determined mainly by the inner unperturbed part of the crown. Hence, under these conditions, the free energy of the entire micelle proves to be equal to that of the isolated micelle with a decreased value of  $N_A$  being the decreasing function of concentration, equation (19).

As has been shown in the preceding section, the number  $f$  of chains in an isolated spherical micelle and the size  $R$  of its core do not have a power law dependence  $N_A$  ( $f, R \sim N_A^0$ ; equation (13) and Table 3). Correspondingly, the minimization of the free energy according to equations (17) and (19) leads to the conclusion that in the concentration range  $c_A^* < c_A < c_A^{**}$  the parameters  $f$  and  $R$  retain the unperturbed values, omitting the logarithmic concentration dependence contained in the coefficient

$$x = \ln(c_A^{**}/c_A) \quad (\text{Table 3})$$

Marked restructuring of the micelle core begins only after the characteristic concentration  $c_A = c_A^{**}$  has been attained. In this case the inner unperturbed layer of the crown disappears ( $\rho = R$ ,  $\Delta F_A^{\text{in}} = 0$ ) and all the space between micelle cores is filled up with a solution of A blocks at a uniform concentration (melt consisting of chains of blobs). As already mentioned, near  $c_A = c_A^{**}$  these blocks grafted onto the micelle cores retain residual extension (at  $N_B > N_A^{1/2}$ ). Then according to equation (22) we have

$$\Delta F_{A,\text{el}}^{\text{ex}} = \Delta F_{A,\text{el}}^{\text{ex}} \simeq \frac{f \xi_A}{R} \simeq \frac{R^2}{a^2 N_B} c_A^{-\nu/(3\nu-1)} \quad (23)$$

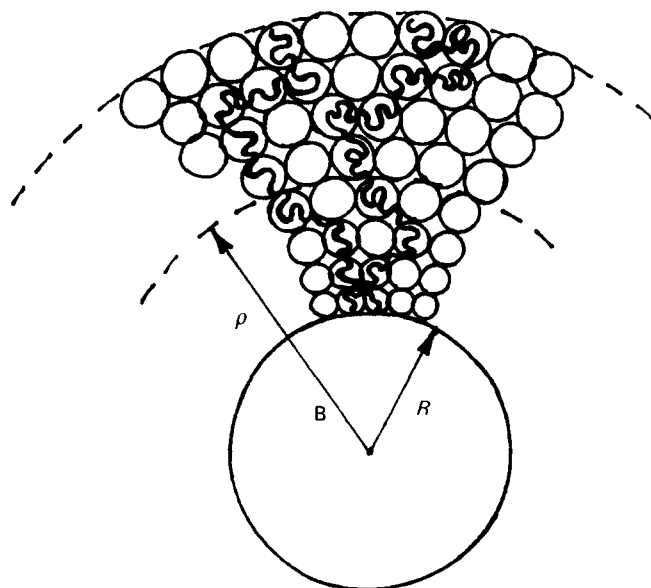


Figure 5 Blob picture of a perturbed layer of a spherical micelle in the concentration range  $c_A^* < c_A < c_A^{**}$

Equation (23) takes into account the fact that  $f \approx R^3/a^2 N_B$ . It can be seen from comparisons of equations (4) and (23) that in this concentration range, just as at lower  $c_A$  values,  $\Delta F_A > \Delta F_B$  and the micelle structure is determined by a compromise between  $\Delta F_S$  from equation (2) and  $\Delta F_A$ , the latter value being dependent on concentration. Hence the characteristics of the micelle core at  $c_A > c_A^{**}$  given in Table 3 are functions of concentration (in contrast to what is observed at  $c_A < c_A^{**}$ ). With increasing concentration, the chain number in the micelle,  $f$ , and correspondingly the size of the dense core,  $R \approx a(N_B f)^{1/3}$ , increase and the specific surface area,  $\sigma = R^2/f \approx N_B/R$ , decreases. The molecular-weight dependences of these characteristics also change: the dependences of  $f$  and  $R$  on  $N_B$  become stronger, in particular  $R \sim N_B^{2/3}$ .

As to the micelle size as a whole, at  $c_A > c_A^*$ , when the system is represented by a set of swollen micelles contacting each other but not interpenetrating (segregated micelles), the dependence of  $D$  on  $c_A$  acquires a 'quasiglobular' character<sup>15</sup>:

$$D \approx f^{1/3} N_A^{1/3} c_A^{-1/3} \quad (24)$$

This dependence is valid both at  $c_A < c_A^{**}$ , where  $f \sim c_A^0$ , and at  $c_A > c_A^{**}$ , where the chain number in the micelle increases with  $c_A$  ( $f \sim c_A^{v/(3v-1)}$ ), so that the resulting decrease in the overall micelle size becomes less marked,  $D \sim c_A^{-1/12}$  at  $v=3/5$  and absent at  $v=1/2$  (Table 3). At  $c_A > c_A^{**}$  the molecular-weight dependence of  $D$  acquires the form  $D \sim (N_B/N_A)^{1/3} N_A^{2/3}$  characteristic of the superstructures of any morphologies at a high polymer concentration (see the forthcoming paper 2 in this series).

Note that the analysis of the micellar structure at  $c_A > c_A^{**}$  proceeded from the assumption that the extension of A and B blocks in this concentration range is retained. The values of  $D$  and  $f$  obtained (equation (24) and Table 3) show that this assumption is valid when the condition  $N_B > N_A^{1/2}$  is obeyed. As indicated above, this condition is also a condition of extension of blocks A at the lower boundary  $c_A \approx c_A^*$  of the regime under consideration. With increasing concentration the chain number in the micelle increases, the specific surface area  $\sigma$  decreases and hence chain extension is retained in spite of the overall increase in concentration in the micelle crown. It is of interest that in the system polymer A in the same polymer B, the 'polymer' properties of B are apparent only under analogous conditions  $N_B > N_A^{1/2}$ , and at  $N_B < N_A^{1/2}$  polymer B is equivalent to a low molecular weight solvent.

## DISCUSSION

In this section we sum up the main results of the theory and compare them with the theoretical and experimental data for micellar structures available in the literature. Unfortunately, the number of papers containing quantitative results and describing the behaviour of relatively dilute two-block copolymer systems is relatively small, which restricts the possibility of carrying out comparisons.

(1) The micelles of two-block copolymers in a dilute solution should be preferentially spherical in shape. This refers, first, to the case  $N_A > N_B^{(1+2v)/5v}$  ( $v$  is an exponent of size for the soluble block A; the micelle core consisting of block B does not contain the solvent). The increasing micelle asymmetry leads to increasing chain energy proportional to  $\Delta F_A^2 \sim (N_A^v N_B)^{1/(3+v)}$ . Hence the deviation from spherical symmetry decreases with increasing

overall chain size  $N \approx N_A$ . It is for this reason that the shape of micelles of block copolymers should be much closer to the spherical shape than that of micelles formed by oligomer molecules.

(2) It is found that the radius  $R_B$  of a spherical micelle is  $R_B \sim N_B^{0.6}$ . In Reference 18 a micelle model with uniform unit density distribution in the crown was considered. By using the mean-field approximation for the calculation of  $\Delta F_A$  the authors of Reference 18 obtained only a slightly different result  $R_B \sim N_B^{0.64}$  in spite of the fact that the two models differ.

(3) The critical concentration of micelle formation and the critical degree of solvent selectivity should decrease with increasing molecular weight of the two-block copolymer.

(4) With increasing block copolymer concentration, three regimes of micelle behaviour take place consecutively: the regime of dilute micelle solution (0) and regimes (I, II) of dense packing of micelles with a swollen crown. Under regime 0 micelle characteristics are independent of concentration. Under regimes I and II the increase in concentration results in a decreasing crown swelling at a constant (regime I) or increasing with concentration (regime II) chain number in each micelle.

This conclusion of the theory may be compared with the experimental data obtained in Reference 19, in which the spherical domains formed by the PS-PB copolymer ( $M_{PS} = 1.56 \times 10^4$ ;  $M_{PB} = 3.64 \times 10^4$ ) were investigated in tetradecane (good solvent for PB and precipitant for PS) in the range of copolymer volume concentrations  $0.07 < c < 0.55$ . The results show<sup>19</sup> that the concentration range investigated is divided into two,  $0.07 < c < 0.17$  (I) and  $0.17 < c < 0.55$  (II). In each of these ranges the structural parameters are described by power laws with exponents  $R_3 \sim c^\eta$ ;  $D_0 \sim D_3 \sim c^\delta T^\omega$  ( $D_0$  is the structure period). The experimental evaluations of the exponents in these regions (I and II) are given in Table 4 (the value of  $\eta = 0.19$  was obtained from the data in Reference 19).

As can be seen from comparing Tables 3 and 4, the behaviour of the system in regions I and II is described by the dependences obtained in the present paper for  $c_A^* < c_A < c_A^{**}$  and  $c_A < c_A^{**}$ . Thus, in region I, in complete agreement with the theory, for  $c_A < c_A^{**}$  the power dependence of  $R$  on  $c_A$  is absent and we have  $D \sim D_0 \sim c_A^{-1/3}$ . A slightly inferior agreement is observed for the regions  $c_A > c_A^{**}$  and II. The reason for this may be the dependence  $\phi = \phi(c_A)$  at  $c_A > c_A^{**}$ , which we have not taken into account explicitly. Note that at  $c_A < c_A^{**}$  the above analysis predicts the absence of the power dependence  $\phi = \phi(c_A)$ . (The part of the micelle crown adjoining the core is not affected by the perturbing action of other micelles and we have  $\phi(c_A) = \text{const.} \times (c_A)$ ).

Let us estimate the transition concentrations  $c_A^*$  and  $c_A^{**}$ . Under the conditions of a good solvent,  $v=3/5$ , equations (9) and (10) give  $c_A^* = f_3^{2/5} N_A^{-4/5}$  and  $c_A^{**} = (\sigma/a^2)^{-2/3}$ . Proceeding from the experimental values

**Table 4** Theoretical and experimental values of exponents in the dependences  $R \sim c^\eta$ ,  $D \sim c^\delta$ ,  $T^\omega$  (spherical morphology)

	Region I			Region II		
	$\eta$	$\delta$	$\omega$	$\eta$	$\delta$	$\omega$
Experiment <sup>19</sup>	0	-0.33	-0.33	0.19	-0.14	-0.33
Theory	0	-0.33	-0.40	0.25	-0.08	-0.33

of  $(\sigma)^{1/2} = 2.7$  nm and  $f_3 = 170$  (region I in Reference 19) and the characteristic transverse size of chain  $a = 0.5$ – $0.8$  nm and passing to the volume concentration of the copolymer in solution.

$$c = c_A \left( 1 + \frac{M_{PS} \rho_{PB}}{M_{PB} \rho_{PS}} \right)$$

( $\rho_{PB}$  and  $\rho_{PS}$  are the densities of the components), we obtain  $c^* \approx 0.04$ – $0.09$  and  $c^{**} \approx 0.15$ – $0.27$ . These values of  $c^*$  and  $c^{**}$  are also in agreement with the experimental data<sup>19</sup> ( $c \approx 0.17$  corresponds to the boundary between regions I and II; the system loses the long-range order and is destroyed into individual aggregates at  $c \approx 0.07$ ) and confirm our interpretation of experimental data. The experimental values of the temperature exponent are also in reasonable agreement with the theoretical prediction (see Table 4). Recollect that the value of  $\phi$  in Table 3 is the ratio of the surface tension coefficient to the energy  $kT$ .

Experimental data in the concentration range  $c \approx 1$  will be discussed in the forthcoming paper 2 of this series.

#### REFERENCES

- 1 Meier, D. J. *J. Polym. Sci. C* 1969, **26**, 81
- 2 Helfand, E. and Wasserman, Z. R. *Macromolecules* 1976, **9**, 879; 1978, **11**, 960; 1980, **13**, 994
- 3 Birshtein, T. M. *Vysokomol. Soedin.* 1982, **24A**, 2110
- 4 Schaefer, D. W., Joanny, I. F. and Pincus, P. *Macromolecules* 1980, **13**, 1280
- 5 Alexander, S. J. *Phys.* 1977, **38**, 983
- 6 Birshtein, T. M. and Zhulina, E. B. *Vysokomol. Soedin.* 1983, **25A**, 1862
- 7 De Gennes, P. G. 'Solid State Physics', Academic Press, New York, 1978, p. 1
- 8 Zhulina, E. B. and Birshtein, T. M. *Vysokomol. Soedin.* 1985, **27A**, 511
- 9 Zhulina, E. B. *Vysokomol. Soedin.* 1983, **25B**, 834
- 10 Zhulina, E. B. *Vysokomol. Soedin.* 1984, **26A**, 794
- 11 Birshtein, T. M. and Karaev, A. K. *Vysokomol. Soedin.* 1988, in press
- 12 Skvortsov, A. M., Pavlushkov, I. B. and Gorbunov, A. A. *Vysokomol. Soedin.* 1988, **30A**, 503
- 13 Zhulina, E. B., Priamitsin, V. A. and Bopisov, O. V. *Vysokomol. Soedin.* 1988, in press
- 14 Birshtein, T. M., Skvortsov, A. M. and Sariban, A. A. *Macromolecules* 1976, **9**, 88
- 15 Birshtein, T. M., Zhulina, E. B. and Borisov, O. V. *Polymer* 1986, **27**, 1078
- 16 Daoud, M. and Cotton, J. P. *J. Phys.* 1982, **43**, 531
- 17 Semenov, A. N. *Zh. Eksp. Teor. Fis.* 1985, **88**, 1242
- 18 Noolandi, J. and Hong, K. M. *Macromolecules* 1983, **16**, 1443
- 19 Shibayama, M., Hashimoto, T. and Kawai, H. *Macromolecules* 1983, **16**, 16